URSI GASS 2021, Rome, Italy, 28 August - 4 September 2021

Preliminary experimental results for thermal transfer printed chipless RFID tags

Alessandro DiCarlofelice, Emidio DiGiampaolo and Piero Tognolatti
Department of Industrial and Information Engineering and Economics, University of L'Aquila, Via G. Gronchi 18, Loc. Pile, 67100 L'Aquila, Italy

Abstract

A numerical and an experimental study of a thermal transfer printed chipless RFID tag is presented. A good agreement between models and measurements has been achieved. Some drawbacks have been highlighted and discussed.

1 Introduction

In recent years, the research investigation has highlighted the potentiality of chipless RFID tag in different field of applications [1], from item tagging [2] to sensing [3] [4] and security [5]. Nevertheless, many issues have to be still addressed in order to make that technology usable in practical applications. First of all, it is necessary to adopt a mass production technique that is reliable and at very low costs in order to achieve a pervasive use. The manufacturing processes relying on inkjet and roll-to-roll printing reduce the production costs and permit the use of cheap materials like paper and flexible plastic films. On the other hand, that printing process makes use of conductive inks that have reduced conductivity and therefore make the tag more difficult to work. The reading distance is typically short while the spectral signature may show not very deep notches. Moreover, the clutter from adjacent objects camouflages the backscattered signal making difficult to identify the spectral signature.
To remedy the aforementioned limitations, different solutions based on Frequency Selective Surfaces [4], [6] and on Van Atta Array [7], [8] have been found to increase the radar cross section (RCS) response and to extended the read range.
In the presented work we investigate the usefulness of thermal transfer printing to realize chipless tags since it is a very cheap technique widespread used in many industrial and services applications to print labels. We perform a study of the behaviour of simple antennas and tag topologies by comparing results of numerical models to measurements on printed realizations of the simulated models.
The paper is organized as follows. Section I describes the electromagnetic models, while section II shows numerical and experimental results. Some conclusions are addressed.

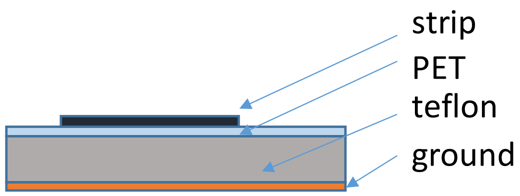

Figure 1. Sketch of the used microstrip structure. Strip: Metallograph ink $\mathbf{250}\,\boldsymbol{nm}$ thick. PET: $50\,\mu m$ thick printing support. Teflon: $5\,mm$ substrate. Ground: $35\,\mu m$ copper.

2 Models and Methods

Models and realized devices are based on microstrip technology having the structure shown in Fig.1. The ground is made with an adhesive sheet of copper having thickness $35\,\mu m$, the substrate is composed of a $50\,\mu m$ foil of polyethylene terephthalate (PET) over a slab of Teflon $1.5\,mm$ thick, the printed structure constitutes the upper layer and is made of Metallograph Alluminum $250\,nm$ thick having nominal bulk conductivity $3.6\cdot 10^{6}\,S/m$ The used thermal transfer printer is Zebra 610T which allows the use of rolls of materials $10.4cm$ large. The design structure is first printed on the PET foil then it is stuck over the Teflon substrate.
We consider four different models useful to determine the goodness of the printing technique for developing chipless tags. The first model is a 50 ohm microstrip line connected at both ends in order to determine the insertion loss. In the second model we introduce a couple of u-shaped resonators tightly coupled to the transmission line in order to evaluate the effectiveness of that kind of resonator in introducing notches in the frequency response. The third model concerns a printed microstrip patch antenna that is used to evaluate the effectiveness of the materials for radiating structures. The patch antenna includes three parasitic elements that behave as additional resonators for increasing the bandwidth. The simulated gain of the antenna is about *5.5 dB*. The fourth model is a chipless tag made with a two elements Van Atta array working in polarization diversity that is realized assembling the transmission line and the patch antennas designed before. The working frequency is in the bandwidth between 3.4 GHz and 3.8GHz envisaging the tag for possible applications in 5G scenarios. The used simulative software is Sim4Life [9].

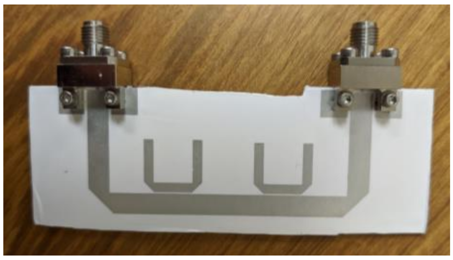

Figure 2. Picture of a printed microstrip line with two u-shaped resonators.

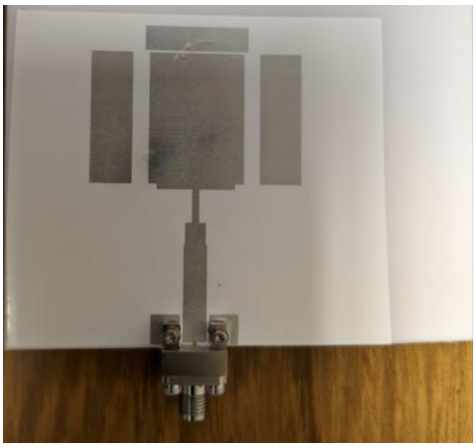

Figure 3. Picture of a printed microstrip patch antenna with parasitic elements for increasing the bandwidth.

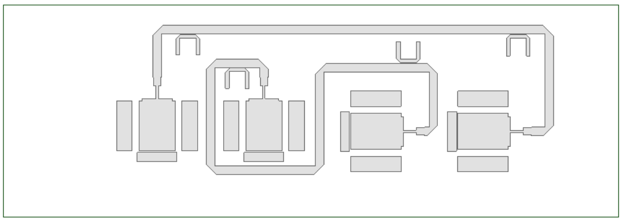

Figure 4. Model of a two-element Van Atta array with microstrip lines and u-shaped resonators.

Figure 5. Picture of the printer workflow.

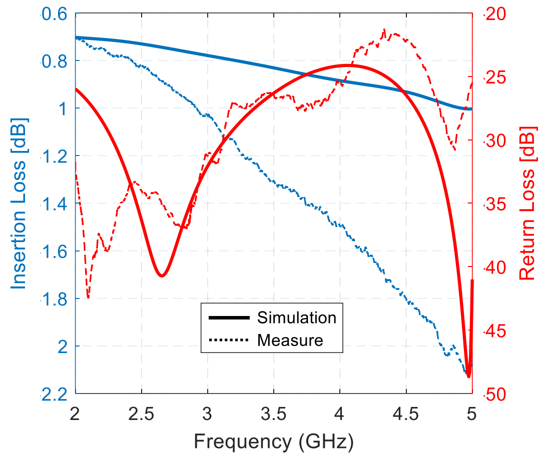

Figure 6. Insertion loss and return loss of the printed microstrip line. Comparison between numerical model and measurements.

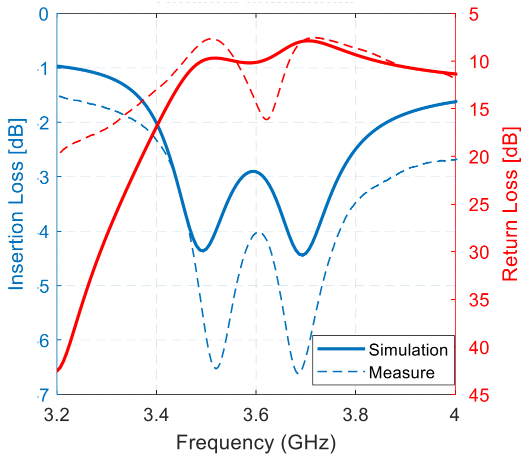

Figure 7. Insertion loss and return loss of the printed microstrip line coupled to two u-shaped resonators. Comparison between numerical model and measurements.

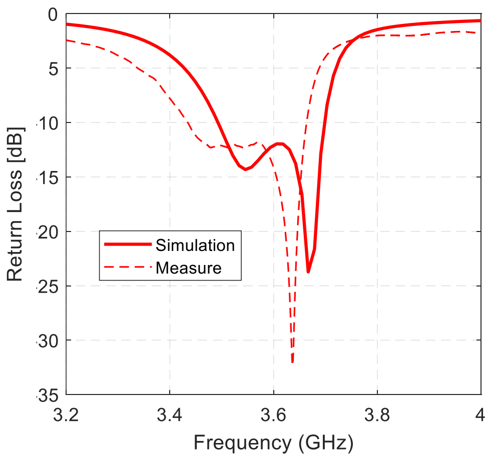

Figure 8. Return loss of the printed microstrip patch antenna. Comparison between numerical model and measurements.

3 Numerical and Experimental Results

A comparison between simulated and measurement results is reported. The insertion loss and return loss of the microstrip transmission line is shown in Fig.1. We observe that the measured insertion loss is less *2dB* in the bandwidth [2 – 5] GHz, it is greater than that simulated but includes the loss of connectors that is not considered in simulation. Losses increase with the frequency as a consequence of the very thin conductive layer of the printed strip. Fig.7 shows the insertion loss and the return loss of the printed microstrip line coupled to two u-shaped resonators. U structures are dimensioned to resonate at 3.5 GHz and 3.7 GHz, evidently a couple of notches are visible at that frequencies, nevertheless the depth of the notches are limited to a couple of dB because of the losses of the printed metallic layer. The position of the peaks of the notches are in agreement with that of simulated model. The return loss of the printed patch antenna is shown in Fig. 8. A part from a small frequency shift due to a discrepancy between the actual and simulated permittivity of the substrate materials, simulations and measurements are in good agreement for what concerns the matched bandwidth. Finally, a two-element Van Atta array made with the line, resonators and patches antenna shown before has been modelled as shown in Fig. 4. Its radar cross section has been calculated by means of simulation considering a plane wave impinging from different directions. In Fig. 9 and in Fig. 10 are reported the simulated results of monostatic radar cross section vs. frequency for impinging angle of 0° and 30°, respectively. A comparison between tags with a without resonators is also shown. The notches introduced by the resonators are clearly visible in both the figures. Notches do not change position by changing the impinging direction, while the level of radar cross section is sufficient high to allow us to hypothesize that tag is readable from sufficient long distance.

4 Conclusion

The overall results obtained in that study make us confident that technology can be profitably used for realizing chipless tags. The major drawback concerns the short depth of the notches that may be camouflaged by noise and clutter, but an optimized design procedure together with a better realization (e.g. including more layers of ink) can overcome that limitation.

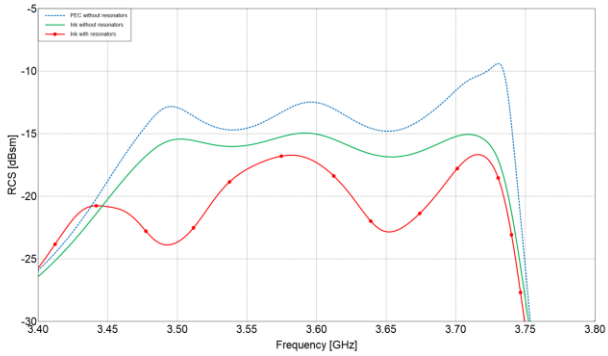

Figure 9. Monostatic radar cross section of chipless tag of Fig.4 for incidence angle of 0°. Continuous blue line: perfect electric conductors condition without u-resonators; green line: conductive ink without u-resonators; dot-marked red line: conductive ink with u-resonators.

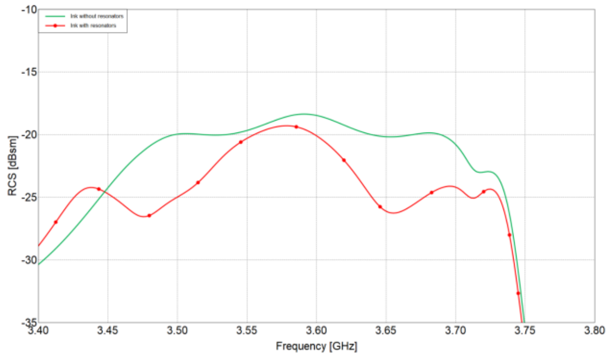

Figure 10. Monostatic radar cross section of chipless tag of Fig.4 for incidence angle of 30°. green line: conductive ink without u-resonators; dot-marked red line: conductive ink with u-resonators.

5 References

1. V. Mulloni, M. Donelli, “Chipless RFID Sensors for the Internet of Things: Challenges and Opportunities”, Sensors 2020, 20, 2135. doi:10.3390/s20072135

2. S. Preradovic, N.C. Karmakar, Design of fully printable planar chipless RFID transponder with 35-bit data capacity, Proc. European Microwave Conference (EuMC) (2009), pp. 013-016. doi:10.23919/EUMC.2009.5296182

3. M. Borgese, F. A. Dicandia, F. Costa, S. Genovesi and G. Manara, "An Inkjet Printed Chipless RFID Sensor for Wireless Humidity Monitoring," IEEE Sensors Journal, vol. 17, no. 15, pp. 4699-4707, 1 Aug.1, 2017, doi:10.1109/JSEN.2017.2712190.

4. Z. Li, S. Bhadra, “A 3-bit fully inkjet-printed flexible chipless RFID for wireless concentration measurements of liquid solutions”, Sensors and Actuators A: Physical, Vol. 299, 2019,111581 doi:10.1016/j.sna.2019.111581.

5. D. Betancourt et al., “Square-shape fully printed chipless RFID tag and its applications in evacuation procedures,” in Proc. 9th EUCAP, Lisbon, Portugal, May 2015, pp. 1–5.

6. D. Betancourt, K. Haase, A. Hübler, F. Ellinger, Bending and folding effect study of flexible fully printed and late-stage codified octagonal chipless RFID tags, IEEE Trans. Anten. Propag. 64 (2016) 2815–2823 doi:10.1109/TAP.2016.2559522

7. A. DiCarlofelice, E. DiGiampaolo and P. Tognolatti, "mm-Wave Chipless RFID Tag for Healthcare Applications," XXXIIIrd URSI/GASS Int. Symposium, Rome, Italy,2020, pp.1-3, doi: 10.23919/URSIGASS49373.2020.9232382.

8. J.G.D. Hester, M.M. Tentzeris, Inkjet-printed flexible mm-wave Van-Atta reflect arrays: a solution for ultralong-range dense multitag and multisensing chipless RFID implementations for IoT smart skins, IEEE Trans. Microwave Theory Techn. 64 (2016) 4763–4773. doi:10.1109/TMTT.2016.2623790.

9. https://zmt.swiss/sim4life/